7th International Congress on Advanced Electromagnetic Materials in Microwaves and Optics – Metamaterials 2013
Bordeaux, France, 16-21 September 2013

Electric Coupling in Strongly-Coupled Magneto-Inductive Cable

R.R.A.Syms[1], T.Floume[1]
[1] EEE Dept, Imperial College London, Exhibition Road, London, SW7 2AZ, UK
r.syms@imperial.ac.uk

Abstract **– Magneto-inductive (MI) waveguides are linear arrangements of magnetically coupled L-C resonators that can propagate RF electrical energy. At resonance, propagation loss is inversely proportional to the coupling coefficients of the elements and to their quality factors. To achieve strong magnetic coupling, the current-carrying sections of adjacent elements must be very close, resulting in parasitic capacitance between elements. Electric coupling is demonstrated theoretically and experimentally in MI cable, and its effect is to introduce multiple propagation bands above the MI band.**

I. INTRODUCTION

Magnetoinductive (MI) waves are current waves that propagate in periodic arrangements of magnetically coupled L-C resonators [1]. They have been observed experimentally [2], and many potential applications have been proposed. Loss is at a minimum at resonance, and high performance requires quality factors and strong magnetic coupling. Flexible magneto-inductive cables combine both properties with immunity to bending, in formats that allow broadband coupling to systems with real impedance [3]. It is generally assumed that the electric fields are confined to the capacitors and hence that the coupling is exclusively magnetic. The possibility of additional electric coupling has been investigated in studies of microwave split ring resonators [4, 5]. However, for sufficiently high magnetic coupling, the tracks of adjacent elements must be close together, resulting in significant electric coupling even at low frequencies. The aim of this paper is to describe the effect of electric coupling on MI cables, and show that it inserts additional pass-bands.

II. THEORY

Fig. 1a shows a magneto-inductive link, consisting of N resonant elements between a source and a load. Ignoring loss, non-nearest neighbour coupling and parasitic effects, the current I_n in the n^{th} element of the periodic section of the line at angular frequency ω is related to the currents I_{n-1} and I_{n+1} by [1]:

$$(j\omega L + 1/j\omega C)I_n + j\omega M(I_{n-1} + I_{n+1}) = 0 \tag{1}$$

Here L is the inductance, C is the capacitance and M is the mutual inductance between nearest neighbours.

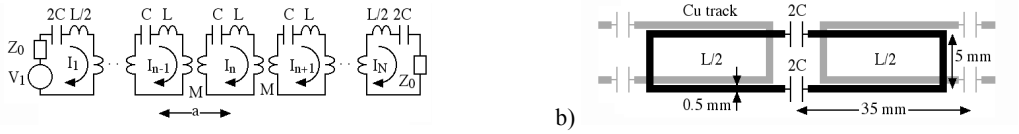

Fig. 1. a) Lumped element circuit for magneto-inductive waveguide, and b) layout of magneto-inductive cable.

Assumption of the travelling wave solution $I_n = I_0 \exp(-jnka)$, where k is the propagation constant and a is the period, then leads to the dispersion equation:

$$\cos(ka) = -(1 - \omega_0^2/\omega^2)/\kappa \tag{2}$$

Here $\omega_0 = 1/\sqrt{(LC)}$ is the angular resonant frequency and $\kappa = 2M/L$ is the magnetic coupling coefficient. Propagation is limited to the frequency range $1/\sqrt{(1 + |\kappa|)} \le \omega/\omega_0 \le 1/\sqrt{(1 - |\kappa|)}$, so the MI waveguide is a band-pass device. Resistive loss in the inductor may be incorporated, by replacing $j\omega L$ with $R + j\omega L$ or alternatively with $j\omega L(1 - j\omega_0/\omega Q_0)$, where $Q_0 = \omega_0 L/R$ is the quality or Q-factor of the elements. Its effect is to render k complex (so that $k = k' - jk''$), introduce propagation loss and allow out-of-band propagation. However, for low loss, k' is approximately as in the lossless case, while $k'' \approx 1/\{\kappa Q_0 \sin(k'a)\}$. At resonance, when $k'a = \pi/2$, $k'' \approx 1/\kappa Q_0$, so that strong coupling and high Q-factor are required for low loss.

Fig. 1b shows MI cable. Each loop is formed from printed inductors on a flexible substrate, together with printed or surface mount capacitors. The loops are divided into two halves, each of inductance $L/2$. The capacitors are also divided into two, each of value $2C$. To form a cable, the loops of adjacent elements are overlaid. A lateral offset of one conductor width is used, to minimize electric coupling. High nearest neighbour magnetic coupling is obtained (with κ positive and approaching unity), while non-nearest neighbour coupling is negligible. The characteristic impedance $Z_{0M} = \omega_0 M$ may be made equal to 50 Ω by suitable choice of M and ω_0, and broadband transducers may be constructed by retaining one loop and one capacitor in a halved element. MI cable has the key advantage that the neither the self-inductance nor the mutual inductance are significantly altered if the cable is flexed, providing immunity to bending. However, because the tracks of magnetically coupled elements run so close, there will be parasitic capacitance between them.

Fig. 2a shows a possible equivalent circuit for a MI cable. One complete element is shown, together with the coupled parts of near neighbours. Parasitic coupling is represented using discrete capacitors shunting the tracks of adjacent elements. In the simplest case, we may use four capacitors $C_P/4$ connecting the extremities of each pair of tracks. The total inductance of one resonator is therefore split into six sections. Four inductances $L_C/4$ correspond to the four horizontal track sections while two other inductances $L_{NC}/2$ correspond to the two vertical sections. The inductances are related by $L = L_C + L_{NC}$. For simplicity, we also assume that the majority of the magnetic coupling takes place between the inductors $L_C/4$, and that the inductors $L_{NC}/2$ are not magnetically coupled. Consequently, there is a mutual inductance $M/2$ in each shaded region.

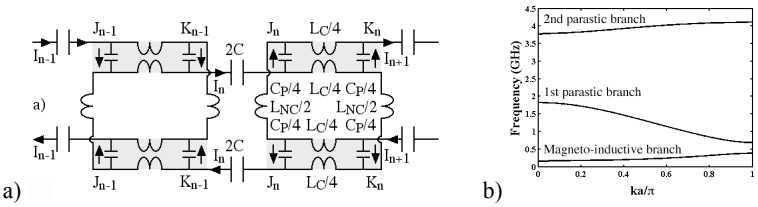

Fig. 2. a) Equivalent circuit model for magneto-inductive cable, and b) simplified dispersion characteristic.

With some manipulation, the dispersion equation may be extracted as:

$$\cos(ka) = -f_1/f_2 \quad \text{with:}$$
$$f_1 = (1 - \omega_0^2/\omega^2)\{(a_1 - a_4^2\omega_0^2/\omega^2)^2 - a_2^2\} - (1 + a_3^2)(a_1 - a_4^2\omega_0^2/\omega^2)/2 + a_2a_3$$
$$f_2 = \kappa\{(a_1 - a_4^2\omega_0^2/\omega^2)^2 - a_2^2]\} - a_3(a_1 - a_4^2\omega_0^2/\omega^2) + a_2(1 + a_3^2)/2$$
$$a_1 = (1 + \alpha)/2;\ a_2 = \alpha + \kappa/2;\ a_3 = \alpha + \kappa;\ a_4 = \omega_{0P}/\omega_0;\ \alpha = L_{NC}/L;\ \omega_{0P} = \sqrt{(8/LC_P)} \tag{3}$$

The model has introduced two new parameters, α (which depends on the inductor arrangement) and ω_{0P} (which depends on the parasitic capacitance C_P). However, when C_P is small, ω_{0P} and a_4 are both large, and we recover Eqn. 2. More generally, we obtain multiple pass-bands. Fig. 2b shows the dispersion characteristic obtained assuming that $f_0 = 227.5$ MHz, $\kappa = 0.66$, $\alpha = 0.07$ and $C_P = 4.3$ pF. Here, experimentally determined parameters have been combined with a value of α obtained from the ratio of the track lengths defining L_{NC} and L, and a value for C_P chosen for agreement with experiment. Three branches may be seen: a MI branch at low frequency, and two parasitic branches at higher frequency. The MI branch is almost identical to the prediction of Eqn. 2, and supports forward waves. In contrast, the first parasitic branch supports backward waves. Increasing C_P forces the first parasitic branch closer to the MI branch, while increasing α mainly alters the separation between the first and second parasitic branches.

The equivalent circuit of Fig. 2a is an extreme simplification. More realistically, the self-inductance inductance, mutual inductance and parasitic capacitance must all be distributed. We have developed more detailed models in which the total parasitic capacitance $C_P/2$ of each pair of tracks is separated into N_C elements distributed along the shaded regions, and the corresponding self- and mutual inductance $L_C/4$ and $M/2$ are subdivided into $N_C - 1$ elements. For $N_C > 2$, the currents in any section of closely-spaced tracks may now vary with distance, due to a combination of magnetic and electric coupling between the two. The effect of the subdivision is to alter the dispersion diagram and the predicted response still further. For every increment in N_C, an additional parasitic band appears at high frequency, and the lower parasitic bands alter slightly. In the limit, the response tends to one in which the transmission matrix of the shaded regions is found by solving the differential equations for an unbalanced two-wire line with additional mutual inductance.

III. EXPERIMENT

Cables were constructed in copper-clad Kapton (35 μm Cu on 25 μm polyimide) with a period a = 35 mm, using inductors measuring 66 mm x 5 mm with a track width of 0.5 mm. The PCB also contained single and paired elements used to extract circuit parameters. The inductance was found by measuring the resonance of a single element tuned with a known capacitance. The Q-factor was found from the 3 dB bandwidth. The mutual inductance and coupling coefficient were found from the resonances of a coupled pair of elements. The following values were obtained: L = 104 nH, Q_0 = 110, M = 34.4 nH and κ = 0.66. Surface mount capacitors (C = 4.7 pF) were used to tune the resonance to the frequency ($f_0 \approx$ 227.5 MHz) giving Z_{0M} = 50 Ω in a cable. Broadband transducers were constructed from halved elements and RF connectors. Ten elements and two transducers (so that N = 12) were overlaid to form a cable 385 mm long. Fig. 3a shows the PCB and a cable.

The full and dotted lines in Fig. 3b show the frequency variation of S_{21} and S_{11} up to 500 MHz. The MI band extends from 200-400 MHz. However, when the frequency range is extended, as shown in the full lines in Figs. 4a and 4b, it is clear that that is at least one additional pass-band that is not predicted by the standard model. The dotted lines in Figs. 4b and 4b show simulations obtained using the model of Fig. 2a, including losses due to the inductors (based in the skin effect) and parasitic capacitors (using a frequency dependent loss tangent). Here, the circuit equations were modified at the input and output transducer, to account for the different local circuit in these loops. For an N-element line, a total of $(N_C + 1)N - N_C$ simultaneous circuit equations were solved. Excellent results are obtained with N_C = 16. In each case, the lowest parasitic band is correctly predicted, together with the peaks and troughs due to standing waves.

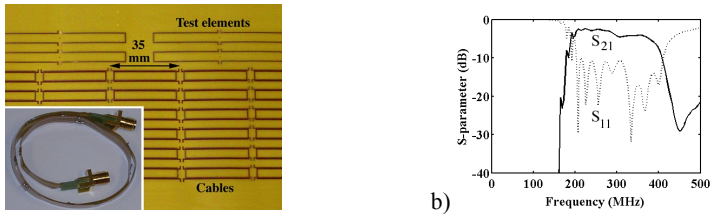

a) b)

Fig. 3. a) Experimental PCB and magneto-inductive cable, and b) low-frequency response.

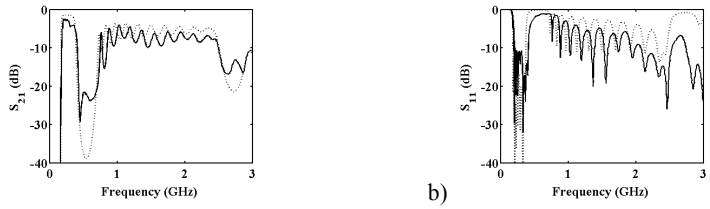

a) b)

Fig. 4. Comparison of experimental response and theory, for a) S_{21} and b) S_{11}.

VI. CONCLUSIONS

Theoretical considerations suggest that electric coupling is likely to be significant in magneto-inductive waveguides, due to the parasitic capacitance introduced when elements are closely overlaid to achieve strong magnetic coupling. These predictions have been confirmed using experiments with magneto-inductive cable.

REFERENCES

[1] E. Shamonina, V.A. Kalinin, K.H. Ringhofer and L. Solymar, "Magnetoinductive waveguide" *Elect. Lett.* vol. 38, pp. 371-373, 2002.

[2] M.C.K. Wiltshire, E. Shamonina, I.R. Young and L. Solymar, "Dispersion characteristics of magneto-inductive waves: comparison between theory and experiment" *Elect. Lett.* vol. 39, pp. 215-217, 2003.

[3] R.R.A. Syms, I.R. Young, L. Solymar and T. Floume, "Thin-film magneto-inductive cables" *J. Phys. D: Appl. Phys.* vol. 43, pp. 425-433, 2010.

[4] V. Lomanets, O. Zhuromskyy, G. Onishchukov and U. Peschel, "Electrical circuit model of arrays of resonant elements" *Phys. Rev. B* vol. 85, 125110, 2012.

[5] F. Hesmer, E. Tatartschuk, O. Zhuromskyy, et al., "Coupling mechanisms for split ring resonators: Theory and experiment" *Phys. Stat. Sol. B* vol. 2044, pp. 1170–1175, 2007.